Available online at www.sciencedirect.com
SCIENCE DIRECT®

Journal of the European Ceramic Society 24 (2004) 2869–2877
www.elsevier.com/locate/jeurceramsoc

Effects of composition and thermal treatment on infrared transmission of Dy-α-sialon

Xinlu Su[a], Peiling Wang[a,*], Weiwu Chen[a], Zhijian Shen[b], Mats Nygren[b], Yibing Cheng[c], Dongsheng Yan[a]

[a]*The State Key Lab of High Performance Ceramics and Superfine Microstructure, Shanghai Institute of Ceramics, Chinese Academy of Sciences, Shanghai 200050, PR China*
[b]*Department of Inorganic Chemistry, University of Stockholm, S-106 91 Stockholm, Sweden*
[c]*School of Physics and Materials Engineering, Monash University, Clayton, Victoria 3800, Australia*

Received 3 March 2003; received in revised form 21 August 2003; accepted 30 August 2003

Abstract

By spark plasma sintering (SPS) and post-sintering thermal treatment at 1700 °C for 7 and 17 h, respectively, the infrared transmissions of Dy-α-sialon with three compositions, $Dy_{0.33}Si_{9.3}Al_{2.7}O_{1.7}N_{14.3}$, $Dy_{0.4}Si_{10.2}Al_{1.8}O_{0.6}N_{15.4}$ and $Dy_{0.67}Si_9Al_3O_1N_{15}$, (abbreviated as Dy1017, Dy1206 and Dy2010, respectively), in 1500–4000 cm^{-1} wave number (6.6–2.5 μ) regions were investigated. The results showed that the second crystallized phase, the sizes of α-sialon grains, the distribution of cations in the grains and the existence of holes on the surface of ceramics were main factors that affected the infrared transmittance of Dy-α-sialon. Among the three SPS-ed specimens, Dy2010 (0.5 mm in thickness) possessed the highest infrared transmission 65%, while those are 58 and 44% for Dy1206 and Dy1017, respectively. Through thermal treatment at 1700 °C for 7 h, the infrared transmittance of Dy2010 and Dy1206 decreased greatly, while that of Dy1017 nearly kept invariable. When thermal treatment time was prolonged from 7 to 17 h, the corresponding infrared transmittance of Dy1206 increased from 37 to 65%. Based on XRD analysis and microstructure observation, the influence of second phase and concentration distribution of cations in the grains on the transmissions of Dy–α-sialon ceramics were discussed.

Keywords: Infrared transmission; Optical properties; Sialons; Thermal treatment

1. Introduction

Since transparences of Al_2O_3 ceramics was reported,[1] many kinds of transparent ceramics such as $MgAl_2O_4$,[2–4] PLZT,[5] AlON,[6,7] and AlN,[8] have been widely and comprehensively studied. In comparison with single crystal and glass, some special advantages of ceramics with translucent property are obvious. Polycrystalline ceramics were easier to be fabricated and produced to larger and more complicated parts than single crystals. Meanwhile they also showed better mechanical and thermal properties than glass, and could overcome the shortcomings of glass that can only be used under 500 °C. Up to now some polycrystalline ceramics have played important role in the different areas, such as transparent polycrystalline Al_2O_3 gas tight envelopes for use in high temperature lamps, particularly those of the arc discharge type;[1] transparent $MgAl_2O_4$ used as transparent armor window material.[9]

According to Beer–Lambert Law, the factors that affect optical transmission of polycrystalline could be divided into intrinsic and extrinsic factors.[10] The intrinsic factors are the characteristics for a specific material that could not be changed, such as strength of bonds and the corresponding vibration energies of the atoms. Varying frequencies of electromagnetic radiation interact differently with the atoms of a material. The radiation can increase the vibrations of the atoms at certain characteristic frequencies or the radiation can excite electrons from filled shells to jump to unfilled higher shell. Both of these phenomena require energy that can be supplied by the incoming incident radiation. Scattering is

* Corresponding author. Tel.: +86-21-5241-2324; fax: +86-21-5241-3122.
E-mail address: plwang@sunm.shcnc.ac.cn (P. Wang).

0955-2219/$ - see front matter © 2003 Elsevier Ltd. All rights reserved.
doi:10.1016/j.jeurceramsoc.2003.08.017

one extrinsic process in which the transmitted wave could be attenuated. Inhomogenieties in the material such as porosity, secondary phases, and grain boundaries, are examples that could scatter a transmitted wave, thus affect the transmission of the material.[11]

α-Sialon (simplified as α′), isostructural with α-Si_3N_4,[12] has an overall composition expressed as $M_xSi_{12-(m+n)}Al_{m+n}O_nN_{16-n}$, where M are alkali and alkaline earth elements such as Li, Ca, Mg or yttrium and most rare earth elements.[13,14] It is well known that α′ exhibits excellent mechanical properties such as hardness and corrosion resistance.[15,16] During sintering process of α′, the added ions $M^{(m/x)+}$ could be absorbed into interstitial site of the α′ lattice, which makes it possible to get the material with clear grain boundary and would be helpful to improve the transmission of α′ ceramics. Combined with its excellent mechanical properties, it is expected that α′ ceramics would play as a promising candidate used as both structural and optical materials at high temperature and under severe conditions, if α′ ceramics with relative high optical transmission could be produced.

In recent years, functional properties of α′ have been paid more and more attention. Karunaratre et al.[17] reported that yellow sialon ceramics with relatively high optical transmission could be prepared by carefully controlling the sintering procedures and using the suitable rare-earth oxides as sintering aids. Shen et al.[18] classified absorption spectra of α′ ceramics according to different doping rare-earth elements. Mandal[19] fabricated some colored and translucent α′ ceramics by capsule-free HIP sintering. Anatoly[20] obtained nearly glass-free materials that are optically translucent (through up to 4 mm thickness samples) based on the starting composition below the α-plane in Nd- and Gd-Si–Al–O–N systems. However, the investigation of effect of compositions and heat treatment on the optical transmission of α′ ceramics is scarce.

The present work mainly focused on Dy–α′ system and studied the effects of different Dy^{3+} content in the compositions and different thermal treatment time with fixed heat treatment temperature that could change the characteristics of grain boundary of α-sialon ceramics, on transmission of Dy–α′ ceramics. It has been known that phase transformation of α′ to β-sialon could occur when α′ is stabilized by rare earth elements, especially light rare earth, and heat-treated at the temperature range of 1000–1500 °C.[21] To avoid the occurrence of transformation and the use of expensive heavy rare earth, the middle heavy rare earth element Dy was considered as a stabilizer to form α′ and 1700 °C was selected as heat treatment temperature in the present work. As mentioned above, ceramics with less grain boundary phase would be beneficial to increase the transmittance of the material. For Dy–α′, the solubility (x value) of α′ is ranged from 0.33 to 0.6.[22] Therefore, the compositions with low m ($m=3x$) as 1.0 and 1.2 were used in the compositions of Dy1017 and Dy1206, respectively. The higher O:N ratio selected in the composition of Dy1017 than that of other two compositions was resulted from the necessary to have enough liquid phase during sintering to densify the material. For comparison, a composition with high m value (Dy2010) was also studied. Furthermore, the reasons that result in the difference in infrared transmission of specimens were also discussed.

In order to study the effect of heat treatment on the optical property of α′ ceramics with three different compositions, it is necessary to have the materials well densified with the uniform distribution of grains. Therefore, a rapid consolidation technique, spark plasma sintering (SPS), was used as the initial sintering way for three samples. Rapid heating rates may have such advantages for α′ ceramics preparation as: (1) the formation of unwanted crystalline intermediate phases could be avoided; (2) the grain growth in the low temperature region could be suppressed; (3) the locally formed liquid would be rapidly homogenized via the large capillary forces present between sub-micrometer and/or nano-sized grains.[23]

2. Experimental

Three compositions Dy1017, Dy1206 and Dy2010 used are located on the α′-plane in the system of Dy-Si–Al–O–N with different m and n values according to the formula of $R_{m/3}Si_{12-(m+n)}Al_{m+n}O_nN_{16-n}$, in which the first composition has the m and n values of 1.0 and 1.7, respectively, and the latter two compositions are lied on the tie line Si_3N_4–9AlN:Dy_2O_3, corresponding to α-sialon compositions of $m=1.2$, $n=0.6$ and $m=2.0$, $n=1.0$ ($m=2n$), respectively.

The initial powders α-Si_3N_4 (SN-10, UBE Industries, Japan, 2.0 wt.%O), AlN (Wuxi Chemical Plant, China, 1.3 wt.%O), Dy_2O_3 (Yaolong Chemical Plant, China, 99.9 wt.%), Al_2O_3 (CR30, Wusong Chemical Plant, China, 99.5 wt.%) were milled in absolute alcohol for 24 h in a plastic jar, using sialon milling media, and then dried under infrared lamp. In the formulation of the composition of Dy1017, the oxygen content on the surface of Si_3N_4 and AlN was taken into account. For the compositions of Dy1206 and Dy2010 that consisted of α-Si_3N_4, AlN and Dy_2O_3 with the different molecular ratios, it is difficult to compensate for oxygen without Al_2O_3 as the starting material, implying that these two compositions will be more oxygen rich. Pellets of dried powders were sintered under nitrogen atmosphere by Dr. Sinter 1050 spark plasma sintering (SPS) apparatus (Sumitomo Coal Co. Ltd., Japan). Compacts were placed between two carbon rams in a cylindrical carbon die with an inner diameter of 20 mm. The pellets were heated with a heating rate of 100 °C/s under 50 MPa

between the rams. The shrinkage and shrinkage rate of specimen were recorded by monitoring the displacement of the rams. When the specimen was not shrinking any more during the SPS process, the temperature was soaking for 75 s, and then the power was taken off. Heat treatment was carried at 1700 °C for 7 and 17 h, respectively in a graphite resistance furnace under protective nitrogen atmosphere. For bulk density comparison, pellets with three compositions Dy1017, Dy1206 and Dy2010 were also hot-pressed at 1800 °C for 2 h with an applied load of 20 MPa in a graphite furnace under a flowing nitrogen atmosphere of 1 atm.

Bulk densities of specimens were measured by Archimedes principle. Phase assemblages were determined by XRD using a Guinier-Hägg camera with Cu $K_{\alpha 1}$ radiation and Si as an internal standard. The measurement of X-ray film and refinement of lattice parameters were completed by a computer-linked line scanner (LS-18) system[24] and the program PIRUM.[25] Microstructure observation was performed under field emissive scanning electronic microscopy (Jeol JSE-6700F). For SEM by second electron mode, the Dy1017 and Dy1206 samples were etched in molten NaOH for seconds before observation. Infrared transmissions in wave number of 1500–4000 cm^{-1} (6.6–2.5 μm) were measured by FT-IR (Nicolet Nexus).

3. Results and discussion

3.1. Properties of specimens after SPS sintering

According to the procedure stated in the experimental section, the sintering temperatures of Dy1017, Dy1206 and Dy2010 during SPS were 1560, 1650 and 1630 °C, respectively, which were strongly related with the oxide content included in the compositions. The higher the oxide content in the compositions is, the lower the SPS temperature used. Bulk densities of specimens after SPS sintering are showed in Fig. 1, in which that of specimens prepared by hot-pressed are also shown. It is noted that the relative densities of the specimens prepared by SPS to that by HP are mostly higher than 99%. If the specimens prepared by HP are considered as fully densified ones, the results of relative densities reveal how powerful of SPS technique is for densification of ceramics as the material could be sintered at such low temperatures even without soak time. The highest bulk density of Dy2010 among three specimens can be understood because of the highest Dy^{3+} amount included in the composition.

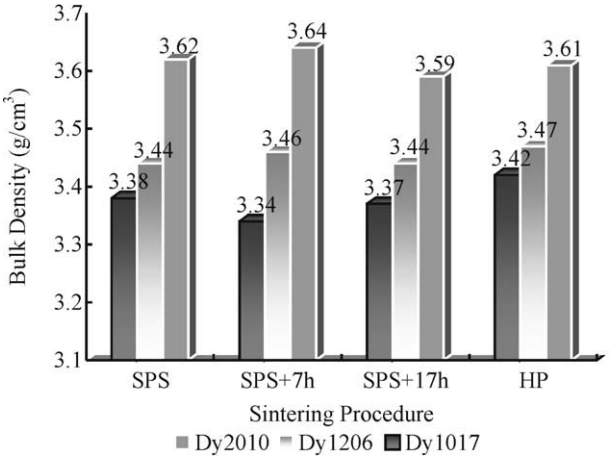

Fig. 1. Dependence of bulk density of Dy–α′ specimens on sintering procedure (SPS: spark plasma sintering; HP: hot-pressing).

The phase assemblages and unit cell dimensions of SPS-ed Dy-α′ specimens are listed in Table 1. Except for a small amount of un-reacted α-Si_3N_4 (about 7 wt.%) in the SPS-ed Dy1017 specimen, which is caused by the relative lower SPS temperature comparing with Dy1206 and Dy2010, the phase assemblages of Dy1206 and Dy2010 samples consist of single α′ phase, which reveals that the formation of α′ phase is mostly completed at such low temperatures (1560–1650 °C) by SPS without soak. The expansion of cell dimensions of α′ phase in SPS-ed Dy1206 and Dy2010 specimens increases with increase of x value in the compositions. However, it is noted that the cell dimensions of α′ phase in SPS-ed Dy1017 are larger than that in Dy1206, although less Dy^{3+} content is contained in the composition of Dy1017 ($x=0.33$) than that of Dy1206 ($x=0.4$), indicating more amount of cations have been incorporated into α′ structure in Dy1017, which is attributed to more liquid phase formed in Dy1017 than that in Dy1206 during the SPS process based on the composition.

SEM micrographs of SPS-ed Dy1017, Dy1206 and Dy2010 are shown in Fig. 2(a)–(c). As shown, the distribution of grain sizes of α′ is homogeneous and the average value of grain sizes of α′ is around 0.5–0.8 μm in the three samples. It is noted however that almost no grain boundaries are observed in Dy1017 and Dy1206 samples and the color is lighter in the center of each α′ grain than that in the margin, implying the distribution of Dy^{3+} in the α′ grain is inhomogeneous and more amount of Dy^{3+} are distributed in the center area of each α′ grain as SEM photos were taken by back-scattering mode. On the other hand, the grain boundary glassy phase, mainly distributed in the triple pockets in SPS-ed Dy2010, has been observed.

The infrared transmission curves of specimens in 1500–4000 cm^{-1} wave numbers (6.6–2.5 μm) are shown in Fig. 3, in which SPS-ed Dy2010 sample has the highest transmittance 65% and SPS-ed Dy1017 has the lowest one 44% among three samples. The lower transmission of SPS-ed both Dy1017 and Dy1206, especially for SPS-ed Dy1017, in comparison to that of SPS-ed Dy2010, is attributed to the inhomogeneous distribution of Dy^{3+} cations in the α′ grains and the appearance of

Table 1
Phase assemblages and cell dimensions of α′ phase in Dy–α-sialon samples

Starting composition	Sintering procedure[a]	Phase composition[b]				Unit cell dimensions		
		α′	M	β′	α	*a* (Å)	*c* (Å)	*V* (Å^3)
Dy1017	SPS	s			w	7.8154(7)	5.7006(8)	301.55
	SPS + HT7h	s		vw		7.8088(4)	5.6920(5)	300.59
	SPS + HT17h	s		vw		7.8081(3)	5.6920(4)	300.54
Dy1206	SPS	s				7.8068(5)	5.6808(7)	299.84
	SPS + HT7h	s	vw			7.8041(5)	5.6847(6)	299.84
	SPS + HT17h	s	tr			7.8039(5)	5.6850(4)	299.85
Dy2010	SPS	s				7.8416(6)	5.7184(7)	304.52
	SPS + HT7h	s	w			7.8372(4)	5.7171(5)	304.11
	SPS + HT17h	s	w			7.8368(5)	5.7164(5)	304.10

[a] SPS = spark plasma sintering; HT = heat treatment at 1700 °C.
[b] α′ = α-sialon, M = melilite, β′ = β-sialon, α = α-Si_3N_4, s = strong, w = weak, vw = very weak, tr = trace.

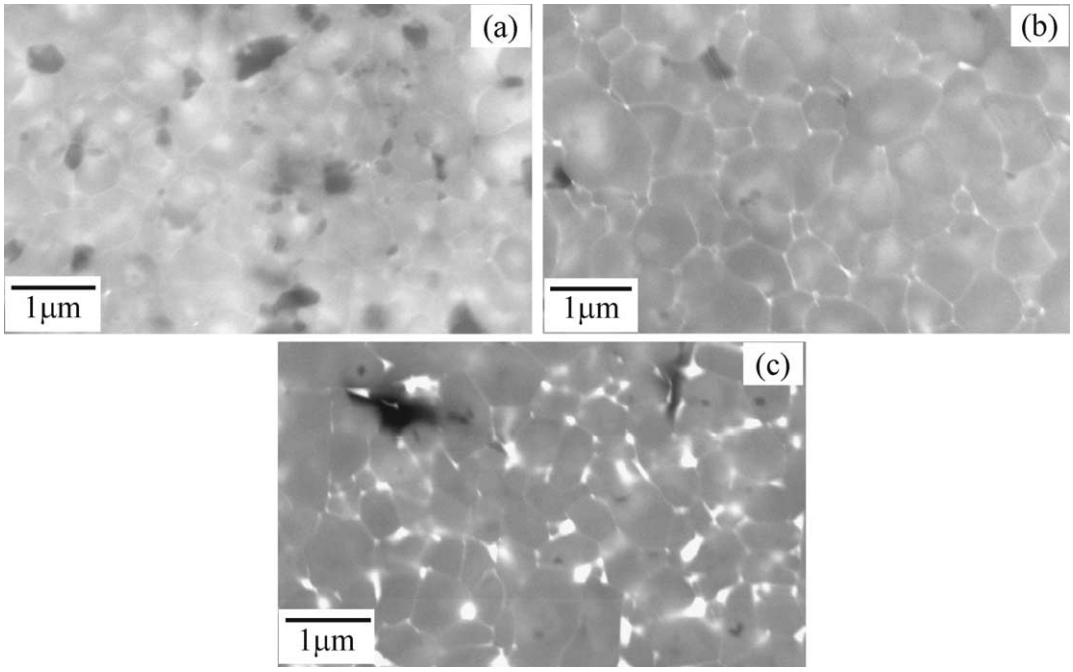

Fig. 2. SEM micrographs by back-scattering mode of (a) Dy1017, (b) Dy1206 and (c) Dy2010 samples after SPS.

un-reacted Si_3N_4 phase in SPS-ed Dy1017. It is noted that each specimen has an absorbing peak edge at about 3500 cm^{-1} wave number that is corresponding to $^6H_{15/2} \rightarrow {}^6H_{11/2}$ electron transition of Dy^{3+}.

3.2. Properties of SPS-ed specimens after thermal treatment

The densities of SPS-ed Dy1017, Dy1206 and Dy2010 specimens after heat treatment at 1700 °C for 7 and 17 h, respectively are shown in Fig. 1. In comparison with the densities before heat treatment, the variation in density after heat treatment is small, which is resulted from the formation of little amount of other phases than α′ during heat treatment.

After thermal treatment for 7 h, small amount of melilite (simplified as M) phase appeared in both Dy1206 and Dy2010 specimens, in which less amount of M was detected in Dy1206 than that in Dy2010. The un-reacted α-Si_3N_4 in Dy1017 disappeared and small amount of β-sialon (simplified as β′) appeared instead. When the thermal treatment time increased for 17 h, amount of the second crystallized phase (M) in Dy1206 decreased, whereas the amount of the second phase in

Dy2010 and Dy1017 were almost unchanged. As concerns cell dimensions of α′ phase in Dy1206 after heat treatment for 7 h, the lattice parameter *c* increased, while *a* decreased, indicating there was distortion in the unit cell of α′ phase, although unit cell volume of α′ phase was nearly invariable. After thermal treatment for 17 h, the cell of α′ phase in Dy1206 kept almost the same as that for 7 h, as the change in cell dimensions was within error of deviation standard. For Dy2010 and Dy1017, the lattice parameters of α′ phase, including *a*, *c* and *v*, decreased after heat treatment for 7, and kept the same values after heat treatment for 17 h. According to the reported results for Y–, Sm– and Ca–α′,[26–28] the absorbed cations caused the cell expansion, which increased linearly with increasing the amount of absorbed cations. The lattice parameters of α′ phase could therefore provide an information of solubility of cations in α′ and reflect, to some extent, the amount of residual grain boundary in the materials. No difference in cell volume of α′ phase between SPS-ed and thermal treated Dy1206 samples implies that there was almost no change in solubility of cations after heat treatment, whereas the solubility of cations decreased obviously after heat treatment in both SPS-ed Dy2010 and Dy1017 specimens, indicating that some Dy^{3+} ions in the α′ grains dissolved into grain boundary after heat treatment.

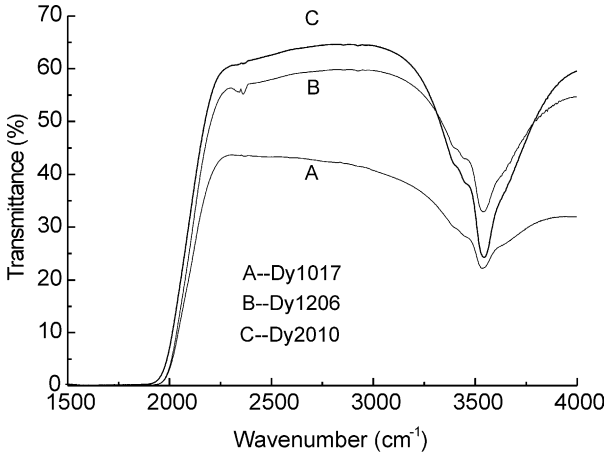

Fig. 3. Infrared transmission of SPS-ed Dy–α′ specimens (0.5 mm in thickness).

As mentioned above that the overall compositions of Dy1206 and Dy2010 lie slightly on the oxygen rich plan side of the α′ plane, as the consequence of not compensation for oxygen, hence resulting in more residual glass in the material. The formation of melilite phase in Dy1206 and Dy2010 specimens after heat treatment could be attributed to the crystallization from grain boundary glassy phase during cooling down.

SEM micrographs of specimens heat treated for 7 and 17 h are shown in Figs. 4(a)–(c) and 5(a)–(d), respectively. As shown in Fig. 4(b), Dy^{3+} in α′ grains is more uniformly distributed in heat treated Dy1206 sample in comparison with that before heat treatment. On the other hand, it can be clearly seen that the intergranular glassy phase in Dy1206 and Dy2010 specimens moved more or less to three-forked grain boundaries gradually during heat treatment. However, the moving rate of intergranular phase in Dy2010 seems to be faster than that in Dy1206, as most of intergranular phase have been gathered up at some three-forked boundaries in

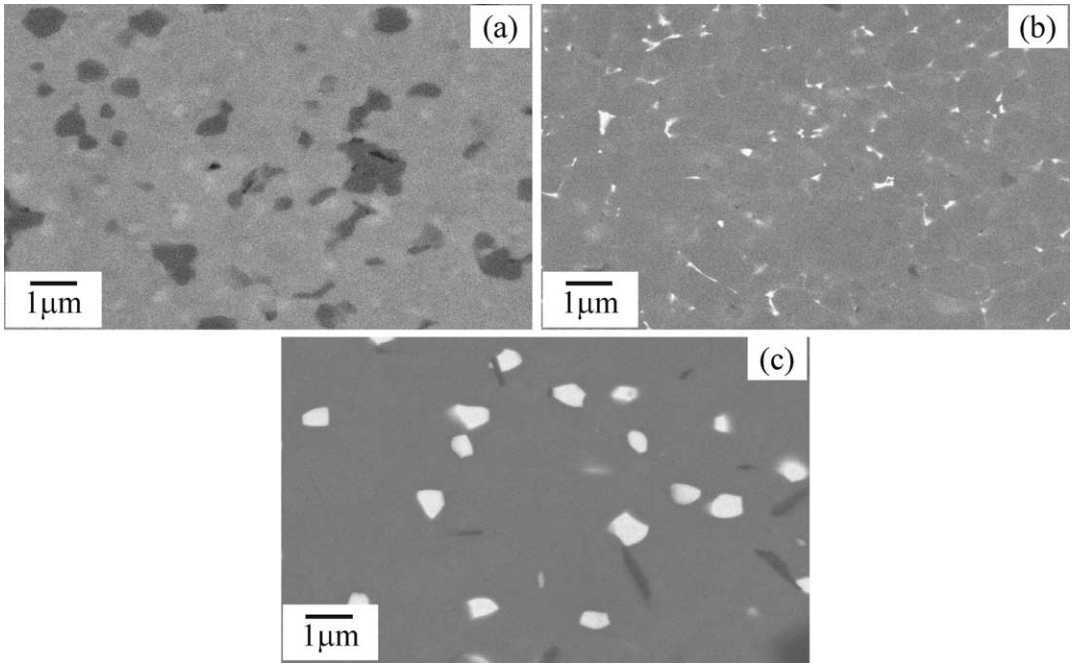

Fig. 4. SEM micrographs by back-scattering mode of (a) Dy1017, (b) Dy1206 and (c) Dy2010 SPS-ed samples after heat treatment at 1700 °C for 7 h.

Dy2010 sample, as shown in Fig. 4(b) and (c). The faster moving rate of intergranular phase may be attributed to enhanced liquid amount and the less liquid viscosity in Dy2010 specimen in comparison with that in Dy1206. During thermal treatment for 17 h, substantial diffusing of cations was still going on. It is noted that there were some enriched Dy^{3+} regions in Dy1206 specimen at last [see white regions in Fig. 5(c)]. The white

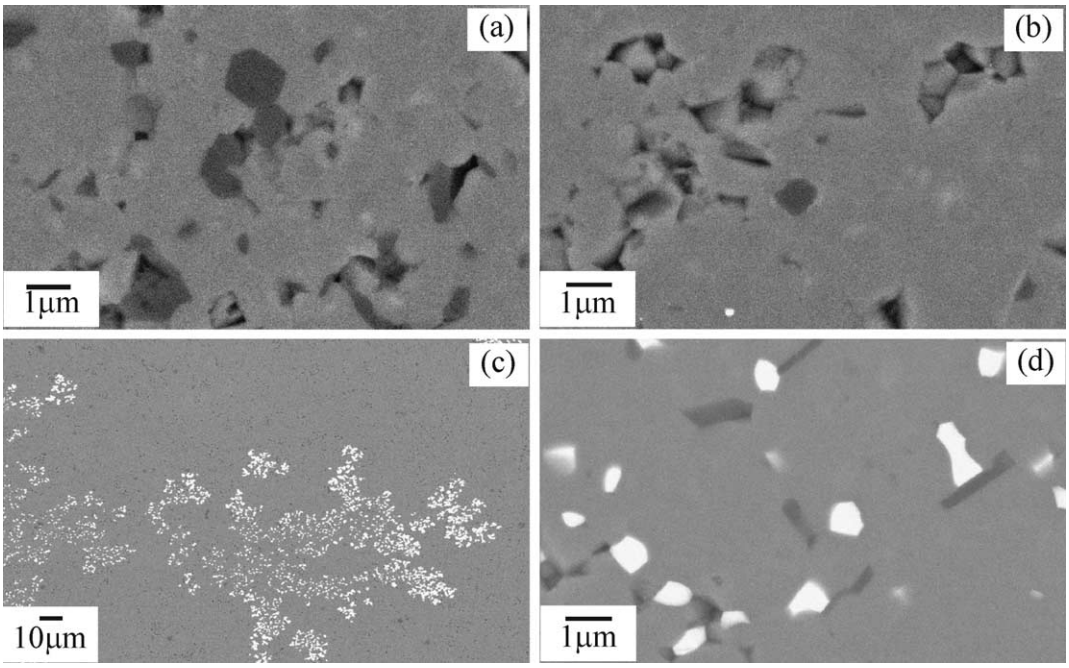

Fig. 5. SEM micrographs by back-scattering mode of (a) Dy1017, (b) Dy1206, (c) enriched region of Dy^{3+} in Dy1206 and (d) Dy2010 SPS-ed samples after heat treatment at 1700 °C for 17 h.

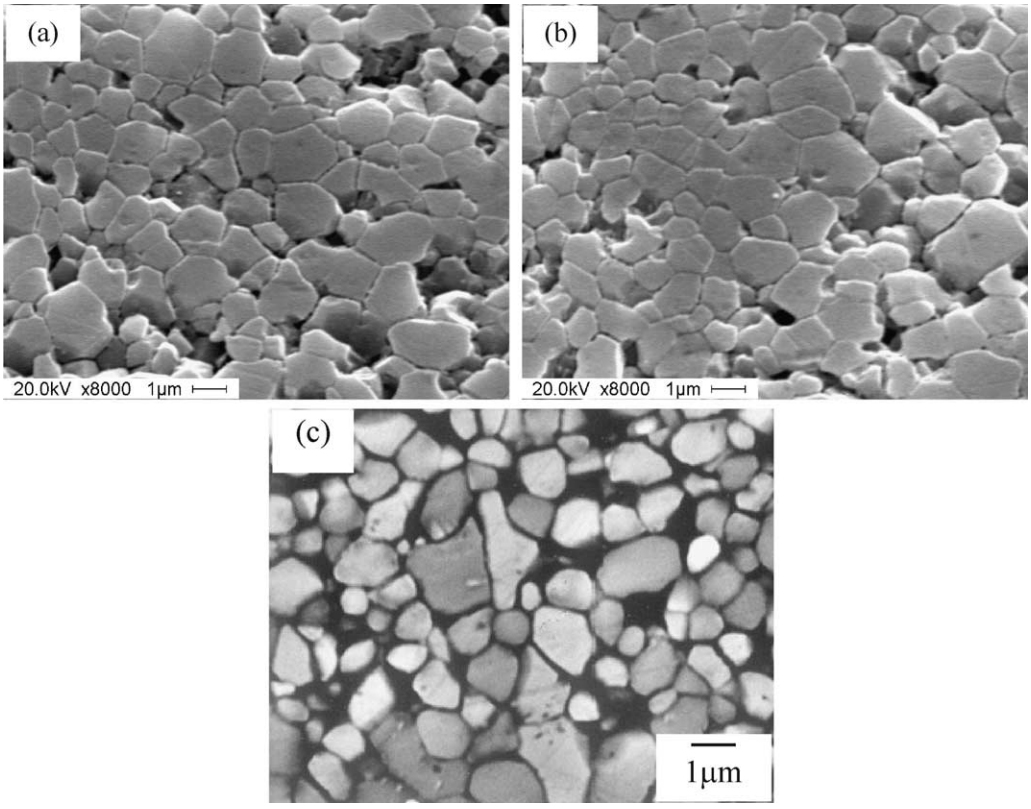

Fig. 6. SEM photographs of heat-treated samples (a) Dy1017 at 1700 °C for 7 h, (b) Dy1017 at 1700 °C for 17 h, (c) Dy1206 at 1700 °C for 17 h.

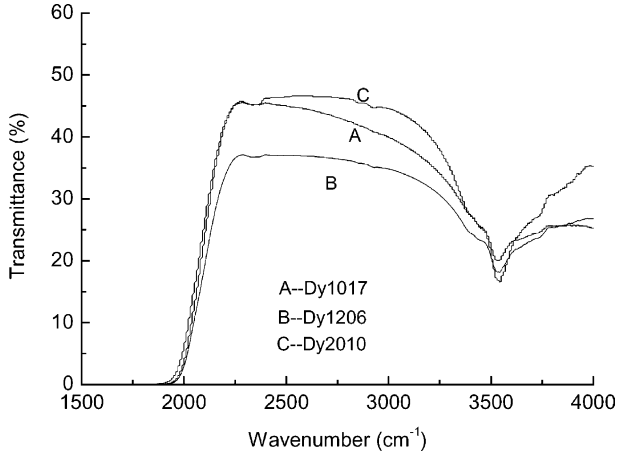

Fig. 7. Infrared rransmission of SPS-ed Dy–α′ specimens after heat treatment for 7 h (0.5 mm in thickness).

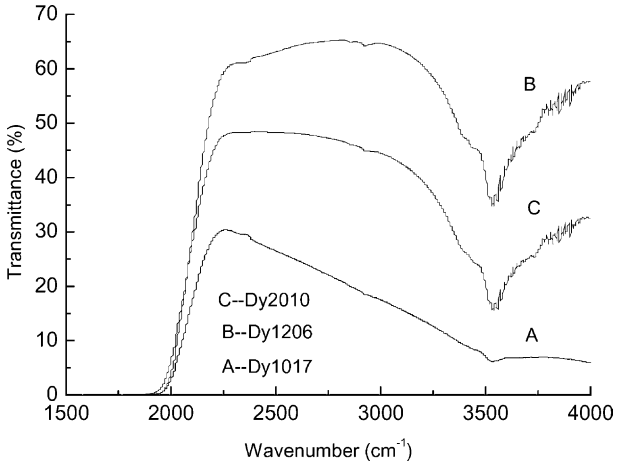

Fig. 8. Infrared rransmission of SPS-ed Dy–α′ specimens after heat treatment for 17 h (0.5 mm in thickness).

Table 2
The maximum values of infrared transmission of Dy–α′ SPS-ed specimens with and without heat treatment

Sample	Maximum of infrared transmission		
	SPS-ed	Heat treated for 7 h	Heat treated for 17 h
Dy1017	44	46	30
Dy-1206	58	37	65
Dy2010	65	46	48

regions are possibly composed of crystallized M and some high viscid glassy phase, which could not move any more. On the other hand, the microstructure of Dy2010 heat treated for 7 and 17 h, as shown in Figs. 4(c) and 5(d) are similar, implying that diffusion of intergranular glassy phase could be completed after heat treated for 7 h. Some elongated grains [see black color in Figs. 4(c) and 5(d)] were observed in both Dy2010 specimens after heat treated for 7 and 17 h by SEM, which were attributed to existence of AlN-polytypoid phase, as it is usually formed in the composition with x higher value and could not detected by XRD because of less enough amount.

Concerning to Dy1017, the amount of Dy_2O_3 contained seems to be insufficiently to well stabilize α′ structure, as β′ phase produced [black regions in Fig. 4(a)] after thermal treatment for 7 h. Prolonging the thermal treatment to 17 h, amount of β′ kept almost the same. It has to be pointed out that many dark holes were observed in Dy1017 and Dy1206 specimens after prolonging the heat treatment for 17 h, as shown in Fig. 5(a) and (b). The holes are likely caused by the residual spaces that the un-firmly bonded grains fall in the course of grinding. It is noted that the appearance of holes occurs in both specimens Dy1017 and Dy1206 under the combined conditions: (1) compositions with lower x values as 0.33 for Dy1017 and 0.4 for Dy1206 in this case, and (2) heat treatment time as long as 17 h, revealing that long thermal treatment time and less liquid phase formed during sintering weaken the bond between grain and grain boundary and result in the occurrence of falling of grains during grinding. It is recognized that there is difficulty to evaluate the sizes of α′ grains after heat treatment by means of SEM micrographs taken by back-scattering mode. The SEM photos by second electron mode for Dy1017 heat-treated for 7 and 17 h and Dy1206 treated for 17 h were therefore taken, as shown in Fig. 6(a)–(c), respectively. It is noted that most α′ grains ranged from 0.5 to 0.8 μm for SPS-ed Dy1017 shown in Fig. 2(a) become larger, not smaller than 1.0 μm, after heat treatment for 7 h. Prolongation of heat treatment to 17 h seems not to be helpful to increase the sizes of the grains. For Dy1206, the prolonged time of 17 h encourages the grain growth of α′, as most grains increase the size from ~0.8 μm for SPS-ed sample, ~1.0 μm for heat treated for 7 h to 1.2–1.5 μm for 17 h heat treatment, shown in Figs. 2(b), 4(b) and 6(c), respectively. Most of α′ grains possess equiaxed morphology and no obvious abnormal grain growth is observed.

Infrared transmittance of specimens in 0.5mm thickness after thermal treatment for 7 and 17 h are showed in Figs. 7 and 8, respectively. To make the comparison with that of SPS-ed specimens, the maximum values of infrared transmission of DY1017, Dy1206 and Dy2010 samples are summarized in Table 2. In the SPS-ed specimens, Dy2010 has the highest transmission (65%) and Dy1017 has the lowest (44%) among three samples. It is noted that the phase assemblages of SPS-ed three specimens, both Dy1206 and Dy2010 consist of single α′ phase; however Dy1017 contains small amount of unreacted α phase. From SEM observation, it has been seen that the distribution of Dy^{3+} in SPS-ed both Dy1206 and Dy1017 samples are inhomogeneous, as

more amount of Dy^{3+} are located in the center area of each α′ grain. On the other hand, more amount of intergranular glassy phase enriched Dy^{3+} has been found in SPS-ed Dy2010 sample than that in SPS-ed Dy1206 and Dy1017. The highest infrared transmission of SPS-ed Dy2010 among three samples implies that uneven distribution of Dy^{3+} in α′ is the main factor to affect the optical property of the materials other than the amount of glassy phase in grain boundary. The lower transmission of Dy1017 than Dy1206 may also be caused by the existence of un-reacted α phase in SPS-ed Dy1017.

After heat treated for 7 h, the infrared transmission of both Dy1206 and Dy2010 decreased, whereas Dy1017 was nearly invariable. It is noted that M phase appeared in both Dy1206 and Dy2010 specimens after thermal treatment for 7 h and the amount of M phase in Dy2010 is higher than that in Dy1206. The second crystallized M phase in Dy1206 and Dy2010 would act as scattering centers and result in the decrease of optical transmission. As the thermal treatment time increased from 7 to 17 h, the infrared transmission of Dy1206 increased obviously, i.e. the corresponding values from 37 to 65%, whereas that of Dy2010 kept almost the same and that of Dy1017 decrease largely.

As mentioned above, that inhomogenieties such as porosity, secondary phases, grain boundaries, which could scatter the transmitted wave, are important extrinsic factors that affect the optical transmission of polycrystalline. It is expected that heat treatment could be a useful way to enhance the grain growth and reduce the grain boundary phase thus improve the optical property of the material. The increased transmission of Dy1206 after prolonged heat treated time was mainly attributed to the increased grain sizes of α′ and the decreased amount of M phase (from about 4 wt.% for 7 h to 2 wt.% for 17 h) and the reduced grain boundary. It was thought that the transmission of Dy1206 after treated for 17 h might be even better without the occurrence of falling of grains during grinding. In Dy2010, prolonged heat treated time for 17 h has not greatly changed the amount of second M phase and intergranular glassy phase, as confirmed by XRD and SEM, resulting in the similar infrared transmission as that of specimen for 7 h. The results indicated that the appearance of second M phase is a main factor to affect the optical property of Dy-α′ and heat treatment, thus resulting in grain boundary phase moving, would be helpful to improve the infrared transmission of α′ material if the appearance of the second M phase in the specimen could be inhibited. It is therefore necessary to tailor the composition and heat treatment properly to get the α′ ceramics with better transmission. For Dy1017 sample, different thermal treated time has not changed the microstructures and the phase assemblage; the decrease in the infrared transmission could only be ascribed to the existence of holes caused by falling of grains in the course of grinding.

It is noted that the cutting frequency of the optical transmittance spectra of three heat treated specimens are all located at about 2000 cm^{-1} (5.0 μm), which is the same as that in SPS-ed specimens, as shown in Figs. 3, 7 and 8, respectively. Each curve has an obviously absorb peak at 3500cm^{-1} due to the existence of Dy^{3+} in the specimens.

4. Conclusions

Dy-α-sialon ceramics with high densification and even grain size distribution can be obtained by SPS sintering at low temperature without soak, which could be used as initial specimens to study their optical properties. There are several factors that affect the infrared transmission of Dy–α′ specimens, i.e. the uniform of distribution of Dy^{3+} in the α-sialon grains, the sizes of α′ grains, the second crystallized phase and the occurrence of holes on the surface. Therefore the infrared transmission of Dy–α-sialon ceramics is a combined result and it is necessary to tailor the composition and heat treatment properly to get the α-sialon ceramics with better infrared transmission. The thermal treatment at 1700 °C is helpful to make Dy–α-sialon ceramics with the uniform distribution of cations in the grains and gather up the intergranular glassy phase into three-forked boundary, resulted from the diffusion of cations. After SPS sintering, Dy2010 specimen (0.5 mm in thickness) showed the highest infrared transmission with the maximum value 65% in 1500–4000 cm^{-1} wave number (6.6–2.5 μ) regions among three specimens. The lowest transmittance of Dy1017 (44%) among three specimens is attributed to the inhomogeneous distribution of Dy^{3+} cations in the α′ grains and the appearance of un-reacted Si_3N_4 phase. After thermal treatment at 1700 °C for 7 h, the infrared transmission of Dy2010 and Dy1206 decreased greatly because of the appearance of melilite phase, whereas that of Dy1017 kept almost invariable (46%) as the one of SPS-ed Dy1017. As thermal treatment prolonged to 17 h, the infrared transmission of Dy1206 increased from 37% for 7 h to 65% for 17 h, which is attributed to the increased sizes of α′ grains, the decreased amount of melilite phase and less intergranular phase resulted from grain boundary moving.

Acknowledgements

This work was supported by The Outstanding Overseas Chinese Scholars Fund of Chinese Academy of Sciences and National Natural Sciences Foundation of China.

References

1. Coble, R. L., *Transparent Alumina and Method of Preparation*. US Pat. 3026210, 10, Mar. 1962.
2. Becher, P. F., Press-forged Al_2O_3-rich spinel crystals for IR applications. *J. Am. Ceram. Soc.*, 1977, **56**, 1015–1017.
3. Maguire, E. A., Richard, J. R. and Gentilman, L., Press forging small domes of spinel. *J. Am. Ceram. Soc.*, 1981, **60**, 255–256.
4. Richard, J. R. and Gentilman, L., Fusion-casting of transparent spinel. *J. Am. Ceram. Soc.*, 1981, **60**, 906–909.
5. Kong, L. B., Ma, J., Zhang, T. S. and Zhang, R. F., Transparent lead lanthanum zirconate titanate ceramics derived from oxide mixture via a repeated annealing process. *J. Mater. Res.*, 2002, **17**, 929–932.
6. Cauley Mc, James W. and Corbin, N. D., Phase relations and reaction sintering of transparent cubic aluminum oxynitride spinel (AlON). *J. Am. Ceram. Soc.*, 1979, **62**, 476–479.
7. Cheng, J. P., Agrawal, D., Zhang, Y. J. and Roy, R., Microwave reaction sintering to fully transparent aluminum oxynitride (AlON) ceramics. *J. Mater. Sci. Lett.*, 2001, **20**, 77–79.
8. Kuramoto, N. and Taniguchi, H., Transparent AlN ceramics. *J. Mater. Sci. Lett.*, 1984, **3**, 471–474.
9. Patel, P. J., Gilde, G. A., Dehmer, P. G. and McCauley, J., W, Transparent ceramics for armor and EM window applications. *Proceedings of SPIE*, 2000, **4102**, 1–14.
10. Mark, F., *Optical Properties of Solids*. Oxford University Press, New York, 2001.
11. Patel, Parimal J., *Processing and Characterization of Aluminum Oxynitride Ceramics*. PhD Thesis, Baltimore, MD, June, 1999.
12. Hampshire, S., Park, H. K., Thompson, D. P. and Jack, K. H., α'-Sialon ceramics. *Nature*, 1978, **274**, 880–882.
13. Huang, Z. K., Sun, W. Y. and Yan, D. S., Phase relations of the Si_3N_4–AlN–CaO system. *J. Mater. Sci. Lett.*, 1985, **4**, 255–259.
14. Thompson, D. P., The crystal chemistry of nitrogen ceramics. *Mater. Sci. Forum*, 1989, **47**, 21–42.
15. Mitomo, M., Tanaka, H., Muramatsu, K., Ji, N. and Fujii, Y., The strength of α-sialon ceramics. *J. Mater. Sci.*, 1980, **15**, 2661–2662.
16. Ekström, T. and Nygren, M., SiAlON ceramics. *J. Am. Ceram. Soc.*, 1992, **75**, 259–276.
17. Karunaratne, B. S. B., Lumby, R. J. and Lewis, M. H., Rare-earth-doped α'-sialon ceramics with novel infrared properties. *J. Mater. Res.*, 1996, **11**, 2790–2794.
18. Shen, Z. J., Nygren, M. and Halenius, U., Absorption spectra of rare-earth-doped α-sialon ceramics. *J. Mater. Sci. Lett.*, 1997, **16**, 263–266.
19. Mandal, H., New developments in α-sialon ceramics. *J. Eur. Ceram. Soc.*, 1999, **19**, 2349–2357.
20. Rosenflanz, A., Controlling grain-boundary phases in α-sialon containing material. *Key Engineering Material*, 2003, **237**, 11–20.
21. Mandal, H., Thompson, D. P. and Ekström, T., Reversible $\alpha \leftrightarrow \beta$ sialon transformation in heat-treated sialon ceramics. *J. Eur. Ceram. Soc.*, 1993, **12**, 421–429.
22. Huang, Z. K., Tien, T. Y. and Yan, D. S., Subsolidus phase relationships in Si_3N_4–AlN-rare earth oxide systems. *J. Am. Ceram. Sci.*, 1986, **69**, C241–C242.
23. Shen, Z. J., Formation of tough interlocking microstructures in silicon nitride ceramics by dynamic ripening. *Nature*, 2002, **417**, 266–269.
24. Johansson, K. E., Palm, T. and Werner, P.-E., An automatic microdensitometer for X-ray powder diffaction photographs. *J. Phys. E. Sci. Instrum.*, 1980, **13**, 1289–1291.
25. Werner, P.-E., A fortran program for least-squares refinement of crystal-structure cell dimensions. *Arkiv fur Kemi.*, 1964, **31**, 513–516.
26. Wang, P. L., Zhang, C., Sun, W. Y. and Yan, D. S., Characteristics of Ca–α-sialon—phase formation, microstructure and mechanical properties. *J. Eur. Ceram. Soc.*, 1999, **19**, 553–560.
27. Sun, W. Y., Tien, T. Y. and Yen, T. S., Solubility limits of α'-sialon solid solutions in the system Si,Al,Y/N,O. *J. Am. Ceram. Soc.*, 1991, **74**, 2547–2550.
28. Shen, Z. J., Ekström, T. and Nygren, M., Temperature stability of samarium-doped α-sialon ceramics. *J. Eur. Ceram. Soc.*, 1996, **16**, 43–53.